nature nanotechnology

SUPPLEMENTARY INFORMATION

DOI: 10.1038/NNANO.2016.3

Chiral atomically thin films

Cheol-Joo Kim, A. Sánchez-Castillo, Zack Ziegler, Yui Ogawa, Cecilia Noguez and Jiwoong Park

List of Supplementary Items

DOI: 10.1038/NNANO.2016.3

Aligned Crystalline Orientation of Graphene

Supplementary Fig. 1a presents optical images of a partially grown single layer graphene film grown for a shorter time. They show hexagonal domains with edges oriented toward a certain direction over the whole area, representing the uniform alignment of crystalline structures, similar to our previous study.[1] More direct structural characterizations are conducted in the fully grown, continuous film by transmission electron microscopy characterization as seen in Supplementary Fig. 1b. The two separated regions, ● and ♦ from the lower left sample were characterized. Both regions show single hexagonal diffraction patterns (selective area: 2,500 μm^2) as seen in the insets, and dark field images in the main panels show continuous films with well aligned crystallinity over the majority of the area (> 95%) without any structural difference, where each colour indicates a specific crystalline orientation (indicated by circles in the diffraction patterns).

Reliability of θ Control in Twisted Bilayer Graphene

Accuracy of θ control is confirmed by observing $\sigma_{inter,\parallel}$ peak energy in the artificially designed twisted bilayer graphene, whose quantitative relation with θ is well known.[2,3] Supplementary Fig. 3a shows a typical $\sigma_{inter,\parallel}$ spectra, obtained by subtracting the σ of Bernal stacked bilayer graphene ($\sigma_{Bernal,\parallel}$) from that of the twisted bilayer graphene ($\sigma_{tBLG,\parallel}$) region (~170 μm^2 area) with θ_{stack} of a 25°. We find that the $\sigma_{inter,\parallel}$ peak appears near the interlayer optical transition energy, E_A (inset, Fig. 2a; main manuscript) for twisted bilayer graphene of $\theta = 25°$, as marked by a triangle.

The uniformity of θ is further confirmed by conducting hyperspectral imaging and large area UV-Vis absorption measurements.[4] Supplementary Fig. 3b shows θ color maps measured from a twisted bilayer graphene made with θ_{stack} of 25°. As the measurement area increases from left to right, one can observe that θ remains within $24° < \theta < 26°$ uniformly over the entire area. Supplementary Fig. 3c shows histograms of θ measured locally by hyperspectral imaging over large areas of four twisted bilayer graphene films with different θ_{stack}. In all twisted bilayer graphene samples, more than 90 % of the area shows $|\theta - \theta_{stack}|$ smaller than 1°.

Interlayer Coupling in Twisted Bilayer Graphene

The interlayer coupling between two stacked graphene is measured by characterizing the spectral weight of the $\sigma_{inter,\parallel}$ peak, resulting from interlayer optical transitions at E_A. As an example, Supplementary Fig. 4 shows $\sigma_{inter,\parallel}$ spectra measured from a pair of twisted bilayer graphene with $\theta = 16.5°$ over 25 mm^2 area (the same samples shown in Fig. 1c; main manuscript). The large area characterization still shows a clear peak near the energy, E_A (marked by a triangle) for θ of 16.5°. The ratio between the spectral weight of the $\sigma_{inter,\parallel}$ peak seen from the fabricated twisted bilayer graphene and that of as-grown twisted bilayer graphene with the same θ remains between 80~90%.[2] The CD signal is normalized by this ratio in order to obtain the intrinsic CD values.

CD Measurement with Change of In-plane Sample Orientation

We have confirmed that the observed ψ originates from intrinsic chiral effects by measuring CD as a function of relative angle, ϕ between the in-plane orientation of the twisted bilayer graphene samples and the polarization of the incident beam. (see Supplementary Fig. 5a) Supplementary Fig. 5b presents the CD spectra taken for six different ϕ from the left-handed (red lines) and right-handed (blue lines) twisted bilayer graphene samples with θ of 16.5°, which remain almost identical for the whole energy range. Supplementary Fig. 5c further shows that the peak CD amplitude at 2.8 eV does not change during a full rotation of the samples, and the sign is only determined by the chirality of the film. These behaviours are consistently observed from other twisted bilayer graphenes with different θ, proving that the CD signals originate from intrinsic chiral effects, not from any other anisotropic light-matter interaction depending on ϕ.

First-principles Calculation of ψ

The light absorption rate in a material can be denoted as a sum of the electric dipole excitation term (Γ_{E1-E1}) and the coupled electric dipole-magnetic dipole excitation term (Γ_{E1-M1}). While achiral Γ_{E1-E1} usually dominates the total absorption, Γ_{E1-M1}, a chirality dependent term, results in CD signals. First, the rate of electric dipole ($\boldsymbol{\mu}$) and magnetic dipole ($\boldsymbol{m}$) excitations can be described as follows.[5,6]

$$\Gamma_{tot} = < E_\alpha \dot{\mu}_\alpha >_\tau + < B_\alpha \dot{m}_\alpha >_\tau , \quad \text{(Eq. 1)}$$

where E and B are the time-dependent applied electric and magnetic fields, respectively, and $<>_\tau$ indicates an average over time.

Using a time dependent perturbation theory, $\boldsymbol{\mu}$ and $\boldsymbol{m}$ induced by the electromagnetic fields on a chiral system is written as[5,6]

$$\mu_\alpha = \alpha_{\alpha\beta} E_\beta - G_{\alpha\beta} B_\beta , \quad \text{(Eq. 2a)}$$

$$m_\alpha = G_{\alpha\beta} E_\beta , \quad \text{(Eq. 2b)}$$

Here, we used the Einstein notation, where α, β are Cartesian coordinate indices. α, G are the complex $\boldsymbol{\mu}$ and the coupled $\boldsymbol{\mu}$-$\boldsymbol{m}$ polarizability tensors, respectively. Circularly polarized light propagating along the direction of $\hat{n}_z$ is given as

$$E = (E^0 / \sqrt{2}) e^{i(kz-\omega\tau)} \left\{ \hat{n}_x \pm i\hat{n}_y \right\}, \quad \text{(Eq. 3a)}$$

$$B = (E^0 / c\sqrt{2}) e^{i(kz-\omega\tau)} \left\{ \hat{n}_y \mp i\hat{n}_x \right\}, \quad \text{(Eq. 3b)}$$

DOI: 10.1038/NNANO.2016.3

where E^0, k, ω are the amplitude, wave vector, angular frequency of the incident light, respectively and τ and c are time and the speed of light. $\hat{n}_x \pm i\hat{n}_y$ in Eq. 3a and $\hat{n}_y \mp i\hat{n}_x$ in Eq. 3b are for right-handed and left-handed polarizations, respectively.

When the polarizabilities of the material are isotropic within the plane perpendicular to $\hat{n}_z$ ($\alpha''_{xx} = \alpha''_{yy}, G'_{xx} = G'_{yy}$), applying Eq. 2 and 3 to Eq. 1 generates Γ_{E1-E1} and Γ_{E1-M1} as follows.

$$\Gamma_{E1-E1} = \omega < |E|^2 >_t = (\omega/2)\alpha''_{xx}(E^0)^2, \quad \text{(Eq. 4a)}$$

$$\Gamma_{E1-M1} = G_{xx} < E_x \dot{B}_x - \dot{E}_x B_x >_\tau + G_{yy} < E_y \dot{B}_y - \dot{E}_y B_y >_\tau = \pm k G_{xx}(E^0)^2, \quad \text{(Eq. 4b)}$$

where + and – correspond to left-handed and right-handed lights, respectively. According to the definition of the ellipticity, $\Psi = (I_L - I_R)/2(I_L + I_R) = (\Gamma^{\text{Left}}_{E1-M1} - \Gamma^{\text{Right}}_{E1-M1})/4\Gamma_{E1-E1} = kG'_{xx}/(\omega\alpha''_{xx})$,

$$\Psi = (kt)(G'_{\parallel}/\sigma_{\parallel}), \quad \text{(Eq. 5)}$$

where $\sigma_{\parallel}$ is the real-part of the in-plane optical sheet conductivity ($\sigma_{\parallel} = t\omega\alpha''_{\parallel}$; unit: Ω^{-1}) and t, the thickness of the system toward the light propagating direction. Considering our experimental geometry, t is equal to the thickness of twisted bilayer graphene (t_{BL} = ~6.6 Å), and $G'_{\parallel}$ and $\sigma_{\parallel}$ are the in-plane components of G' and σ of twisted bilayer graphene. This equation, $\Psi = (kt_{BL})(G'_{\parallel}/\sigma_{\parallel})$ is thus used for the analysis of our experimental data in the manuscript.

We further note that $G'/\sigma \sim G'_{\parallel}/\sigma_{\parallel}$ in twisted bilayer graphene because of the strong two-dimensional nature of the optical processes in twisted bilayer graphene. According to our calculations (not shown here), $G'_{\parallel} \gg G'_{\perp}, \sigma_{\parallel} \gg \sigma_{\perp}$ for the same t, due to the highly anisotropic structure of twisted bilayer graphene. Therefore, $\psi = (kt)(G'/\sigma)$

$$= (kt)\left(\frac{2G'_{\parallel} + G'_{\perp}}{3}\right)\Big/\left(\frac{2\sigma_{\parallel} + \sigma_{\perp}}{3}\right) \approx (kt)(G'_{\parallel}/\sigma_{\parallel}).$$

To calculate $G'_{\parallel}$ and $\sigma_{\parallel}$, the twisted bilayer graphene systems are modelled as infinite two-dimensional films constructed by repeating a unit cell with periodicity. Starting from a Bernal-stacked graphene bilayer, we construct twisted bilayer graphene by rotating the upper layer about the overlapping sublattice by θ. In certain θ, twisted bilayer graphene becomes commensurate and form a primitive cell if

$$\cos\theta = \frac{n^2 + 4nm + m^2}{2\left(n^2 + nm + m^2\right)}, \quad \text{(Eq. 6)}$$

where n, m are integers. The lattice vectors of the commensurate twisted bilayer graphene supercell, labelled by (n, m), are $\boldsymbol{s}_1 = n\boldsymbol{a}_1 - m\boldsymbol{a}_2$, and $\boldsymbol{s}_2 = -m\boldsymbol{a}_1 + (n + m)\,\boldsymbol{a}_2$, where $\boldsymbol{a}_1$ and $\boldsymbol{a}_2$ are the lattice vectors of the primitive unit cell of single layer graphene.

Using periodic boundary conditions allows the wavefunctions of the periodic system to be represented in terms of the momenta of the particles rather than positions. By using the commutation rule $\left[\vec{r},\hat{H}\right]=(i\hbar/m_e)\hat{p}$, where $\vec{r}$, $\hat{H}$ and $\hat{p}$ are the position, the Hamiltonian and the momentum operators, the *G'* tensor can be written as

$$G_{\rho\rho}=\frac{-q^2}{2m_e{}^3\hbar}\sum_{f\neq i,\rho}\frac{\Gamma_{fi}}{\omega_{fi}}\left\{\frac{P'_{\rho\rho}}{\omega_{\rho f}\left[\left(\omega_{fi}-\omega\right)^2+\Gamma_{fi}^2\right]}-\frac{P''_{\rho\rho}}{\omega_{i\rho}\left[\left(\omega_{fi}+\omega\right)^2+\Gamma_{fi}^2\right]}\right\}, \quad \text{(Eq. 7)}$$

$$P'_{\rho\rho}=\left\langle i|p_\rho|f\right\rangle\left[\left\langle f|p_\nu|\rho\right\rangle\left\langle\rho|p_\lambda|i\right\rangle-\left\langle f|p_\lambda|\rho\right\rangle\left\langle\rho|p_\nu|i\right\rangle\right], \quad \text{(Eq. 8a)}$$

$$P''_{\rho\rho}=\left[\left\langle i|p_\nu|\rho\right\rangle\left\langle\rho|p_\lambda|f\right\rangle-\left\langle i|p_\lambda|\rho\right\rangle\left\langle\rho|p_\nu|f\right\rangle\right]\left\langle f|p_\rho|i\right\rangle, \quad \text{(Eq. 8b)}$$

and $p_{\rho,\nu,\lambda}$, are the Cartesian components of the momentum operator. The matrix elements, $\left\langle i|p_\rho|f\right\rangle$ correspond to transitions from the ground states $|i\rangle$ to the excited states $|f\rangle$. $\hbar\omega_i$ and $\hbar\omega_f$ are the energies of the ground state and the final state, respectively and $\omega_{fi}=\omega_f-\omega_i$. Here, Γ_{fi} is a dephasing rate between eigenstates, which is taken to be the same for all the electronic states (Γ_{fi} = 0.05 eV in this work).

To compute CD, it is also necessary to have precise knowledge of the atomic configuration existing in the optically active compound under consideration, as well as a reliable methodology to obtain its electronic structure. We employ a linear-scaling density functional theory (DFT) to perform structural optimizations, electronic structure calculations, optical absorption, and chiroptical properties quantification. The theoretical method has been described in previous works.[7–9] For the sake of conciseness, we only discuss the main features of the method. A novel implementation based in a time-perturbed first-principles theory within DFT was developed to calculate CD, which allows us to perform CD calculations for periodic and finite nanostructures composed of several hundred atoms. The optimized atomic structures of twisted bilayer graphene are obtained by using the siesta package[10] that employs numerical atomic orbitals (2s and 2p for Carbon), and a double—ζ polarized basis set.[11] The exchange correlation effects were included through both Perdew and Zunger parametrization local density approximation[12] and the Perdew-Burke-Ernzerhof parametrization of the generalized gradient approximation.[13]

To calculate the electronic density of states (DOS), we perform integrations in the k-space over 12 points, and use a grid of 100 k-points to calculate the optical absorption and CD spectra. Electronic transitions are computed over all occupied and unoccupied states generated by the extended-function basis set, where at least 50 empty bands are considered. These guarantee convergence of the chiroptical properties. DFT calculations are based on the single-particle Kohn-Sham equations, where the electronic gap is underestimated. To overcome this, we open the gap with a constant energy shift of 0.55 eV that does not alter the electronic transitions, *i.e.*, the corresponding CD

DOI: 10.1038/NNANO.2016.3

peaks, their width, intensity, and sign are not affected. Recently, it was shown that the present methodology is an affordable first-principles tool to study CD spectra for systems composed of several tens or even hundreds of atoms of different species. Particularly, it was found to agree remarkably well with our experimental results quantitatively for carbon nanotubes.[9]

Supplementary Fig. 6 shows the calculated DOS, $\sigma_{tBLG,\parallel}$ and CD spectra of right-handed twisted bilayer graphene for $\theta = 21.8^{o}$. We observe two sharp peaks in the $\sigma_{tBLG,\parallel}$ spectrum at the energies of E_A and E_B (inset, Fig. 2a; main manuscript) as marked by dotted lines. The $\sigma_{tBLG,\parallel}$ peak positions are in good agreement with the CD peak positions as they are correlated with each other in the experimental data.

We note that there could be an electric quadrupole excitation related contribution to the CD signals in oriented chiral samples as in our case, however such contributions have been found much weaker than those from the coupled $\boldsymbol{\mu}$-$\boldsymbol{m}$ interaction in other chiral films with the same symmetry of our films.[5] Indeed, the CD spectra calculated solely based on the coupled $\boldsymbol{\mu}$-$\boldsymbol{m}$ interaction without the consideration of the quadrupole term reproduces the experimental data well both qualitatively and quantitatively as mentioned in Fig. 3 of the main text, suggesting that the coupled $\boldsymbol{\mu}$-$\boldsymbol{m}$ interaction is the main source of the CD effects we observe.

Estimation of Circular Birefringence Spectra

The CD spectra of twisted bilayer graphene can be converted to optical rotation (a) spectra, referred to also as circular birefringence spectra, using Kramers-Kronig relations as described below.[5]

$$\alpha(\lambda) = \frac{2}{\pi}\int_0^\infty \frac{\Psi(\lambda')\lambda'}{\lambda^2 - \lambda'^2} d\lambda' , \quad \text{(Eq. 9)}$$

where λ is the wavelength of the light. Here, we assume that Ψ is zero outside of our spectrum range (190 nm-800 nm). Supplementary Fig. 7 shows the calculated circular birefringence spectra of six chiral pairs of twisted bilayer graphene (black: left-handed, grey: right-handed) with different θ, corresponding to the CD data shown in Fig. 2a of the main text. Two main features are observed. First, every spectra shows oscillating features whose sign is flipped near the interlayer resonance energies, E_A (marked by a triangle) and E_B (a diamond). Here, the highest α value in each spectra is close to the highest Ψ value in the corresponding CD spectra. Second, the entire circular birefringence spectra changes its sign (but not the shape) for the opposite handedness of twisted bilayer graphene with the same θ, similar to the CD cases. While direct experimental measurements of α are still required in order to fully understand the circular birefringence phenomenon in twisted bilayer graphene, this estimation will provide a useful information for future studies.

CD Effect from Natural Chiral Molecules and Metamaterials

Supplementary Table 1 shows the list of molar volume, molar ellipticity, ellipticity per unit thickness and the peak wavelength for several chiral molecules. In order to estimate the maximum CD effect from chiral molecules, we assume a pure film, whose density is the same as that of the constituting chiral molecules. Here, the CD values are taken at the optical resonance energies of the chiral molecules. We also add CD data measured from artificially fabricated metamaterials for comparison.

DOI: 10.1038/NNANO.2016.3

References

1. Brown, L. *et al.* Polycrystalline graphene with single crystalline electronic structure. *Nano Lett*. **14**, 5706–5711 (2014).

2. Havener, R. W., Liang, Y., Brown, L., Yang, L. & Park, J. Van Hove singularities and excitonic effects in the optical conductivity of twisted bilayer graphene. *Nano Lett.* **14**, 3353–3357 (2014).

3. Moon, P. & Koshino, M. Optical absorption in twisted bilayer graphene. *Phys. Rev. B* **87**, 205404 (2013).

4. Havener, R. W. *et al.* Hyperspectral imaging of structure and composition in atomically thin heterostructures. *Nano Lett.* **13**, 3942–3946 (2013).

5. Barron, L. D. *Molecular Light Scattering and Optical Activity*. (Cambridge University Press, Cambridge, 2009).

6. Yang, N. & Cohen, A. E. Local geometry of electromagnetic fields and its role in molecular multipole transitions. *J. Phys. Chem. B* **115**, 5304–5311 (2011).

7. Sánchez-Castillo, A. & Noguez, C. Understanding optical activity in single-walled carbon nanotubes from first-principles studies. *J. Phys. Chem. C* **114,** 9640–9644 (2010).

8. Hidalgo, F., Sánchez-Castillo, A. & Noguez, C. Efficient first-principles method for calculating the circular dichroism of nanostructures. *Phys. Rev. B* **79,** 075438 (2009).

9. Noguez, C. & Hidalgo, F. Ab initio electronic circular dichroism of fullerenes, single-walled carbon nanotubes, and ligand-protected metal nanoparticles. *Chirality* **26,** 553–562 (2014).

10. Soler, J. M. *et al.* The SIESTA method for ab initio order-N materials simulation. *J. Phys.: Condens. Matter* **14,** 2745–2779 (2002).

11. Troullier, N. & Martins, J. L. Efficient pseudopotentials for plane-wave calculations. *Phys. Rev. B* **43,** 1993–2006 (1991).

12. Perdew, J. P. & Zunger, A. Self-interaction correction to density-functional approximations for many-electron systems. *Phys. Rev. B* **23,** 5048–5079 (1981).

13. Perdew, J. P., Burke, K. & Ernzerhof, M. Generalized gradient approximation made simple. *Phys. Rev. Lett.* **77,** 3865–3868 (1996).

14. Stein, G., Stein, J. & Kleinsmith, L. J. *Methods in Cell Biology, Vol. 18*. (Academic Press, New York, 1978).

15. Matsuo, K. & Gekko, K. Vacuum-ultraviolet circular dichroism study of saccharides by synchrotron radiation spectrophotometry. *Carbohydr. Res.* **339,** 591–597 (2004).

16. Kuwata-Gonokami, M. *et al.* Giant optical activity in quasi-two-dimensional planar nanostructures. *Phys. Rev. Lett.* **95,** 227401 (2005).

17. Gibbs, J. G., Mark, A. G., Eslami, S. & Fischer, P. Plasmonic nanohelix metamaterials with tailorable giant circular dichroism. *Appl. Phys. Lett.* **103,** 213101 (2013).

DOI: 10.1038/NNANO.2016.3

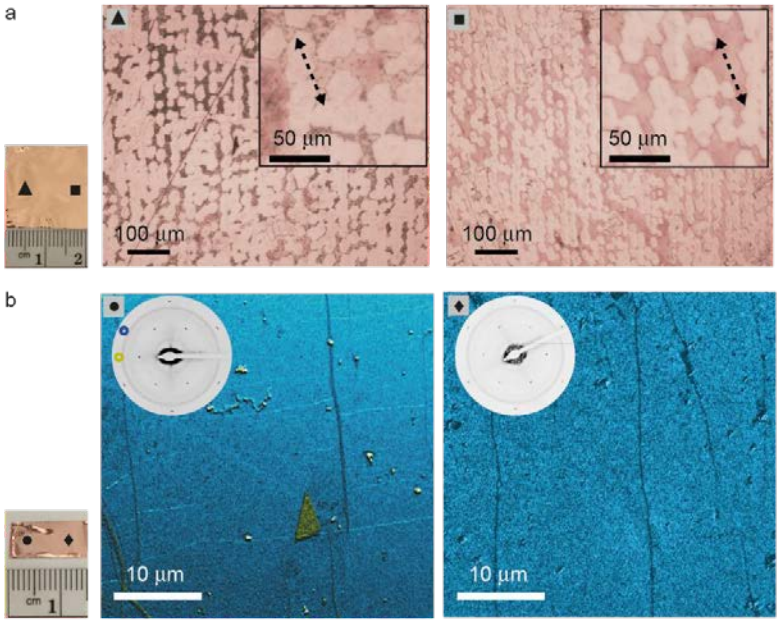

Supplementary Figure 1 | Graphene film with aligned crystallinity. a, Optical images of an partially grown graphene sample. The direction of domain edges is indicated by dotted arrows for comparison in the insets. **b,** Transmission electron microscopy data from fully grown graphene film. Inlets show diffraction patterns (selective area: 2,500 μm^2), and main panels show dark field images.

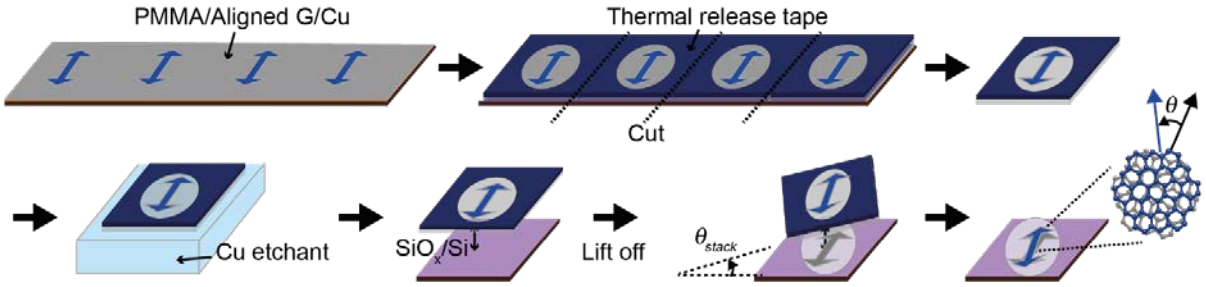

Supplementary Figure 2 | Schematics for the chiral stacking process.

DOI: 10.1038/NNANO.2016.3

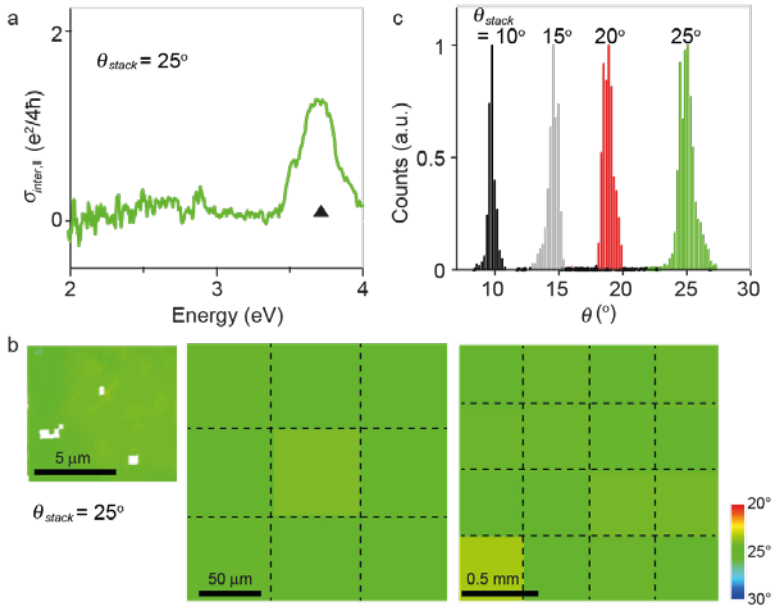

Supplementary Figure 3 | Optical characterization of reliability of θ control. a, Interlayer optical conductivity spectra measured from the twisted bilayer graphene with θ_{stack} of 25°. The interlayer optical peak appears at the expected peak position, marked with a triangle. **b,** Colour map of θ in twisted bilayer graphene with θ_{stack} of 25°. The left image presents data from a zoomed-in area with diffraction limited resolution, and the middle and the right images (pixelated) were generated based on data from 9 and 16 local measurements respectively, taken over a larger area. **c,** Histograms of optically measured θ by hyperspectral imaging over four different twisted bilayer graphene films with different θ_{stack} (10°, 15°, 20°, 25°).

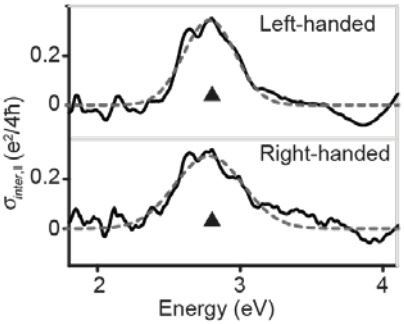

Supplementary Figure 4 | Optical characterization of interlayer coupling. $\sigma_{inter,\parallel}$ spectra of left-handed and right-handed twisted bilayer graphene with $\theta = 16.5°$ with expected peak positions marked by triangles. The dashed lines are Gaussian fitting based on the experimental data (solid lines) in order to deduce the spectral weight of the peaks, which show 80~90% of that of as-grown twisted bilayer graphene with same θ.

DOI: 10.1038/NNANO.2016.3

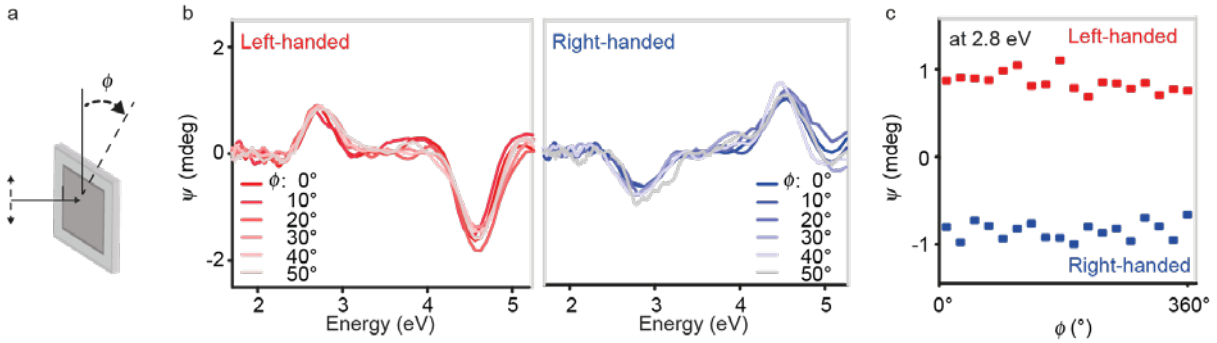

Supplementary Figure 5 | CD measurement with change of in-plane sample orientation. a, Schematics for CD measurements. **b,** CD spectra for left-handed (red lines) and right-handed twisted bilayer graphene (blue lines) with θ of 16.5° for different sample rotation, ϕ. **c,** CD peak amplitudes at 2.8 eV as a function of ϕ.

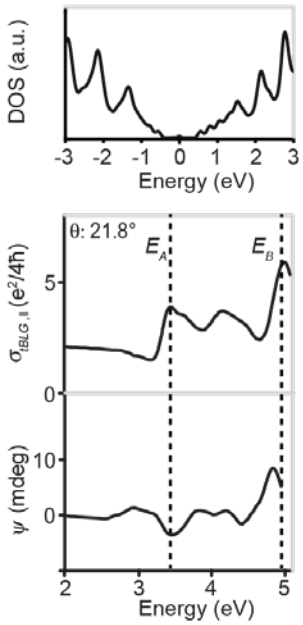

Supplementary Figure 6 | Calculated optical spectra of twisted bilayer graphene. Calculated density of states (top), $\sigma_{tBLG,\parallel}$ (middle) and CD spectra (bottom) of right-handed twisted bilayer graphene for $\theta = 21.8^{o}$.

DOI: 10.1038/NNANO.2016.3

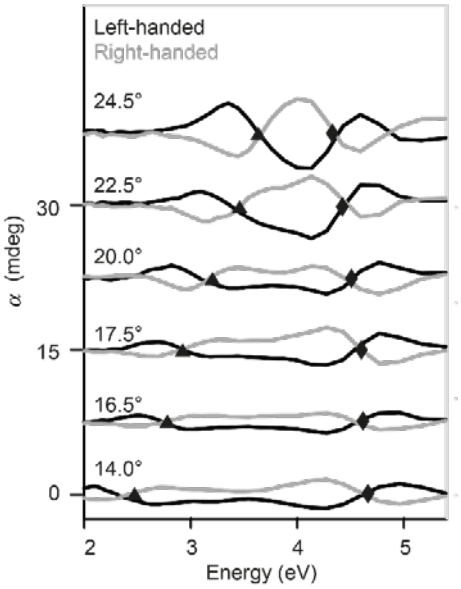

Supplementary Figure 7 | Estimated circular birefringence spectra of twisted bilayer graphene. Estimated circular birefringence spectra of chiral twisted bilayer graphene pairs with different θ (black: left-handed, grey: right-handed) calculated using Kramers-Kronig relations and the experimentally measured CD spectra. (Fig. 2a, main text) The spectra are offset by 7.5 mdeg each for clarity. The interlayer resonance energy of E_A (E_B) is marked by a triangle (diamond) in the spectra.

Samples	Volume per Decimole	Molar Ellipticity	Ellipticity per Thickness	Wavelength	Reference #
	$cm^3/dmol$	$deg \cdot cm^2/dmol$	deg/μm	nm	
Twist Bilayer Graphene			6.5	335	Our Experiment
Camphorsulfonic Acid	17.9	7.8	4.4×10^{-5}	290	Ref. 14
D-Glucose	11.7	1.1×10^{4}	9.2×10^{-2}	168	Ref. 15
D-Xylose	9.87	7.1×10^{3}	7.2×10^{-2}	167	Ref. 15
D-Galactose	10.5	-4.6×10^{3}	-4.4×10^{-2}	177	Ref. 15
Maltose	22.2	6.5×10^{3}	2.9×10^{-2}	166	Ref. 15
Planar Metal Structure			9.8	790	Ref. 16
Metallic Nanohelix			60	711	Ref. 17

Supplementary Table 1 | Ellipticity in natural chiral molecules and metamaterials.